

MEMS Deformable Mirrors for Astronomical Adaptive Optics

S.A. Cornelissen¹, A.L. Hartzell¹, J.B. Stewart¹, T.G. Bifano^{1,2}, P.A. Bierden¹

¹Boston Micromachines Corporation, 30 Spinelli Pl, MA 02138,
(617)868-4178, SAC@bostonmicromachines.com, (617)868-8796, PAB@bostonmicromachines.com.

²Boston University, 15 St. Mary's St., Brookline, MA 02446, (617) 353-5619, tgb@bu.edu

1. ABSTRACT

We report on the development of high actuator count, micro-electromechanical (MEMS) deformable mirrors designed for high order wavefront correction in ground and space-based astronomical adaptive optics instruments. The design of these polysilicon, surface-micromachined MEMS deformable mirrors builds on technology that has been used extensively to correct for ocular aberrations in retinal imaging systems and for compensation of atmospheric turbulence in free-space laser communication. These light-weight, low power deformable mirrors have an active aperture of up to 25.2mm consisting of a thin silicon membrane mirror supported by an array of 140 to 4092 electrostatic actuators which exhibit no hysteresis and have sub-nanometer repeatability making them well suited for open-loop control applications such as Multi-Object Adaptive Optics (MOAO). The continuous membrane deformable mirrors, coated with a highly reflective metal film, are capable of up to 6 μ m of stroke, have a surface finish of <10nm RMS with a fill factor of 99.8%. Presented in this paper are device characteristics and performance test results, as well as reliability test data and device lifetime predictions that show that trillions of actuator cycles can be achieved without failures.

2. INTRODUCTION

Microelectromechanical systems (MEMS) based deformable mirrors (DMs) are an emerging class of wavefront correctors used in an expanding field of applications including biomedical imaging, microscopy, pulse shaping, free-space laser communications, and astronomical imaging. These DMs, manufactured using polysilicon surface micromachining processes, are extremely light-weight and compact, consume very little power, and are scalable to arrays of thousands of actuators. Boston Micromachines Corp. (BMC) has developed deformable mirrors with continuous facesheets, piston-only mirror segments, as well as tip-tilt-piston mirror segments, using highly reliable electrostatic actuators with up to 6 microns of stroke and 4092 actuators.

BMC MEMS DMs have been used in many AO test beds for astronomical adaptive optics imaging systems over the past 8 years, and has been demonstrated in on-sky operations in 2007 at the Nickel 1-meter telescope at the Lick Observatory on Mt. Hamilton, in the Visible light Laser Guidestar Experiments (ViLLaGEs) [1,2]. The 3.5 μ m stroke, 140-actuator DM used in this instrument was shown to provide precise atmospheric wavefront compensation, demonstrating diffraction-limited imaging in R through I bands, in both open and closed-loop operation. This MEMS-based adaptive optics system which permanently resides at the observatory has demonstrated the robustness and the feasibility of the use of MEMS DMs in astronomical AO.

Other astronomical AO instruments using MEMS DMs that are currently being constructed, include a low-cost, autonomous, integrated laser adaptive optics system and science instrument called CAMERA [3], due to be deployed on the 1.5 meter telescope at Palomar Observatory later this year, and the Gemini Planet Imager (GPI) that will use a 4092 actuator MEMS DM, scheduled for first-light in 2011 [4-6].

The compact size, light-weight, and low-power consumption characteristics of MEMS DMs have also made these devices enabling components for a number of space-based astronomical high-contrast imaging systems and both the 1020 actuator continuous facesheet device and 331 segment tip-tilt-piston device are currently in testbeds for these instruments. A 1027 segment tip-tilt-piston DM with 3081 actuators for NASA's visible nulling coronagraph instrument is currently under development for imaging and spectroscopy of Exo-planets [7,8].

In this paper we present device performance characteristics and data on the reliability of these deformable mirrors, and the roadmap to >4092 actuator-count devices for the next generation of astronomical telescopes.

3. CONTINUOUS FACESHEET DMS

Boston Micromachines' MEMS deformable mirrors are based on the surface-micromachined, poly-silicon double cantilever actuator architecture illustrated in figure 1. The device structure consists of actuator electrodes underneath a double cantilever flexure, the actuator, which is electrically isolated from the electrodes and maintained at a ground potential. The electrostatic actuators are arranged in a square grid and the flexible mirror surface is connected to the center of each actuator through a small attachment post that translates the actuator motion to a mirror surface deformation.

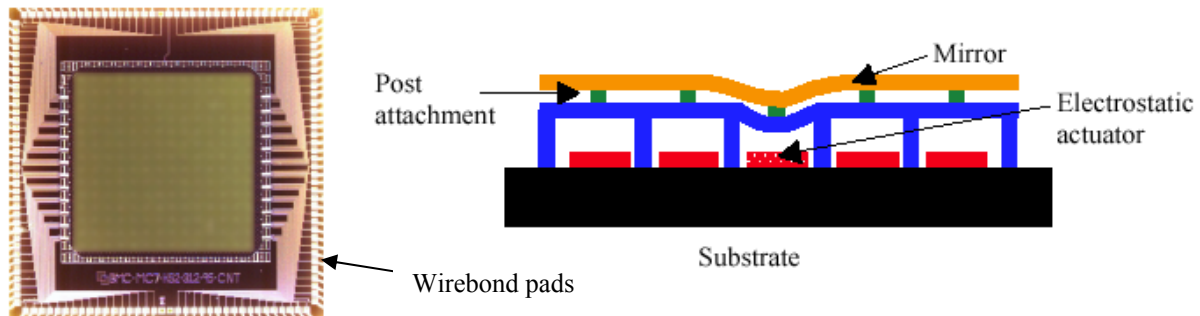


Figure 1. Cross-section of 1x5 electro-statically actuated MEMS deformable mirror.

The devices are fabricated using batch polysilicon surface micromachining processes using photolithographic and chemical etching techniques to pattern and form the device structural materials, making the scaling of the DMs to larger arrays straightforward since the actuator geometry can simply be repeated on the CAD generated mask set. As the number of actuators grows, however, the number of wire traces needed to control the applied voltage at the actuator electrode increases accordingly. Since conventional wirebonding techniques are used to make the electrical interconnects between the silicon DM die and its ceramic chip carrier, all wire traces need to be routed to the periphery of the DM substrate, as shown in Figure 1. This means scaling up from a 32x32 actuator DM to a 64x64 actuator DM, with active apertures of 92mm² and 370mm² (4X increase) respectively, results in a substrate size increase of 8X – 290mm² to 2300mm². As a result, fewer devices can be manufactured in a fabrication run and each DM becomes more susceptible to microscopic manufacturing defects. Both of these factors reduce the overall yield and have been the focus of significant effort over the past few years during the development of the 4092 actuator MEMS DM. Although a 100% actuator yield for a MEMS device of this size and larger is quite possible to achieve, developing all the processes to meet the electromechanical and optical performance requirements as well as actuator yield in only a few batch process fabrication runs presents a significant challenge. A typical MEMS product device development cycle that may deal with device sizes of only a few millimeters on a side, may require dozens of fabrication runs to work out design and fabrication process bugs to achieve high-yielding devices. Although this

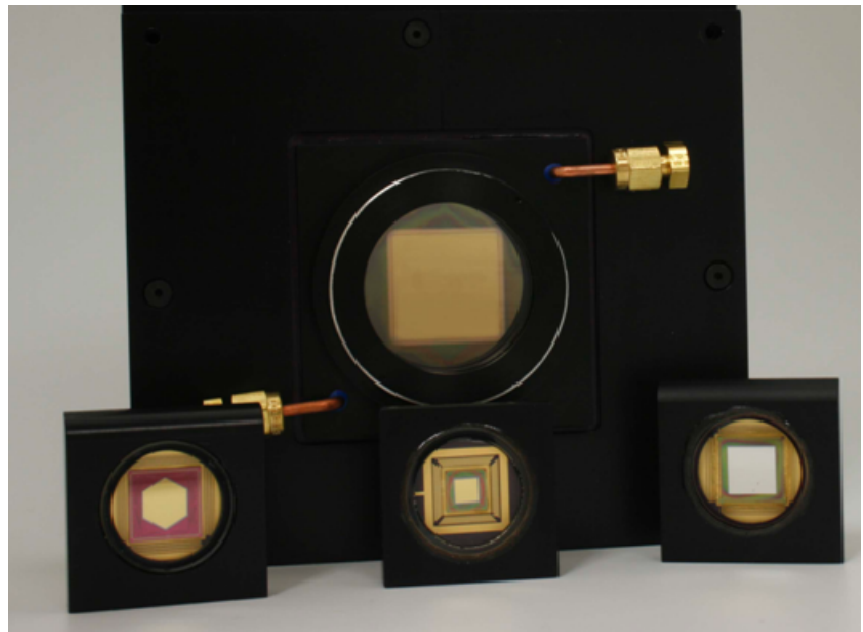


Figure 2. Boston Micromachines MEMS deformable mirrors including the 140, 1020, and 4096 actuator continuous facesheet, and 331 segment (993 actuator) tip-tilt-piston DMs

process development requires significant funding, once the process has been proven, many devices can be manufactured in a single run and can be provided at significantly lower cost than macroscale or hand-assembled counterparts.

Continuous facesheet MEMS DMs with 32, 140 and 1020 actuators have been developed using this architecture (see Figure 2) and are now routinely manufactured with 100% actuator yield. The highest actuator yield achieved to date for a 4092 actuator DM is 99.4%. This DM had 25 anomalous actuators that were either not-responsive, coupled electrically to other actuators, or did not achieve the full deflection when powered.

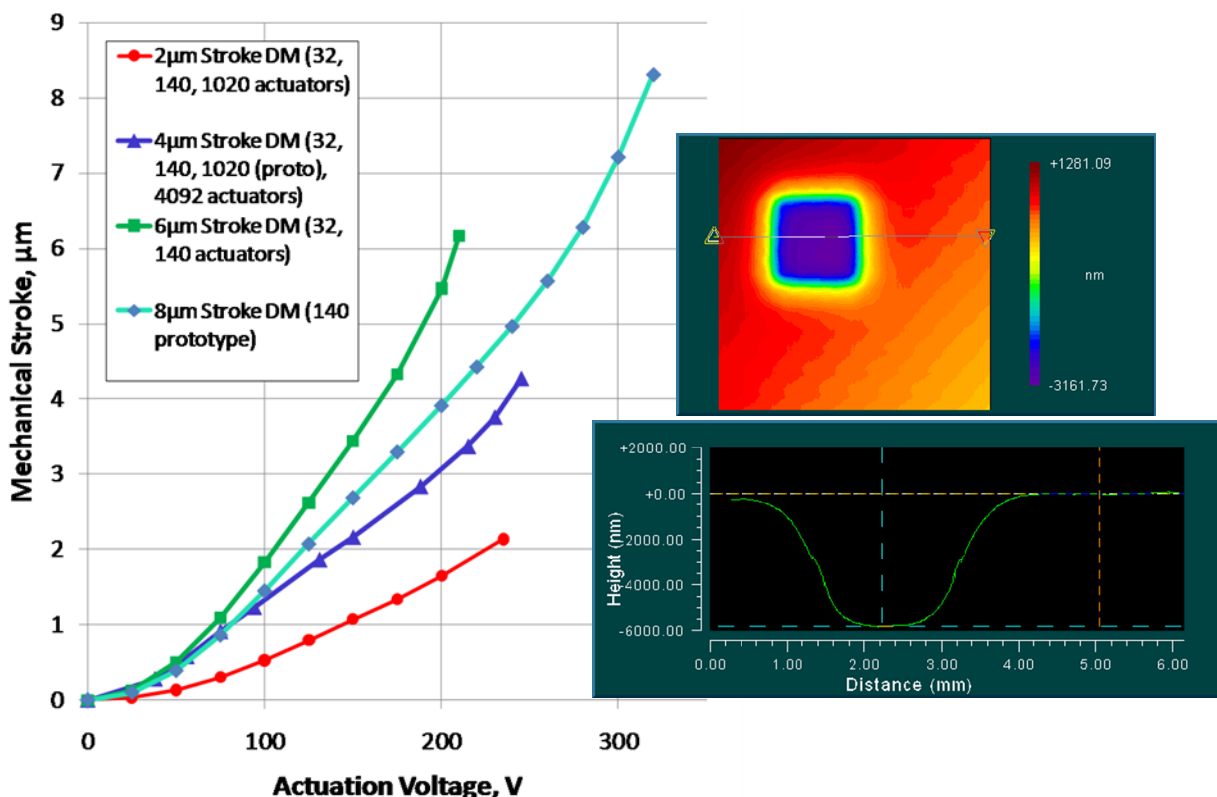


Figure 3. Electromechanical performance of BMC MEMS DM actuators capable of 2, 4 and 6 μ m of stroke. An 8 μ m stroke device has also been demonstrated (left). Actuator stroke is measured in the center of a 4x4 actuator subaperture as shown on the surface map and profile (right)

Electrostatic actuator designs have been developed to meet the needs of varying applications, with 2 μ m, 4 μ m, and 6 μ m of mechanical stroke, although to ensure reliable operation, the operating range is reduced by 0.5 μ m so that it can operate with a significant margin over snap-through – an irreversible actuator failure-mode that occurs when the gap between the actuator flexure and its electrode is small enough that equilibrium between the electrostatic and mechanical restoring force is no longer achievable. Prototype devices with over 8 μ m of stroke have been demonstrated as well. Figure 3 shows the non-linear nature of the electromechanical performance of these devices that is inherent in all MEMS deformable mirrors using parallel plate-type electrostatic actuators.

The DM architecture shown in Figure 1, allows for local deformation of the mirror membrane with an influence function from 11-25% depending on the specific device design. Influence function, defined as the ratio of the deflection induced on a neighbor of a powered actuator and the maximum deflection of the powered actuator, with all other actuators at half bias, for the three different DM actuator types is shown in Figure 4. These profile measurements of the DM surfaces at half bias with an actuator pulled down and poked up show the influence functions of these devices to be 15%, 13%, and 22% for the 1.5, 3.5, and 5.5 μ m stroke DM actuator types respectively.

The DM architecture that produces these localized influence functions makes these wavefront correctors well suited to correct for high order aberrations in the optical path of imaging systems, such as those associated with atmospheric turbulence encountered in astronomical imaging.

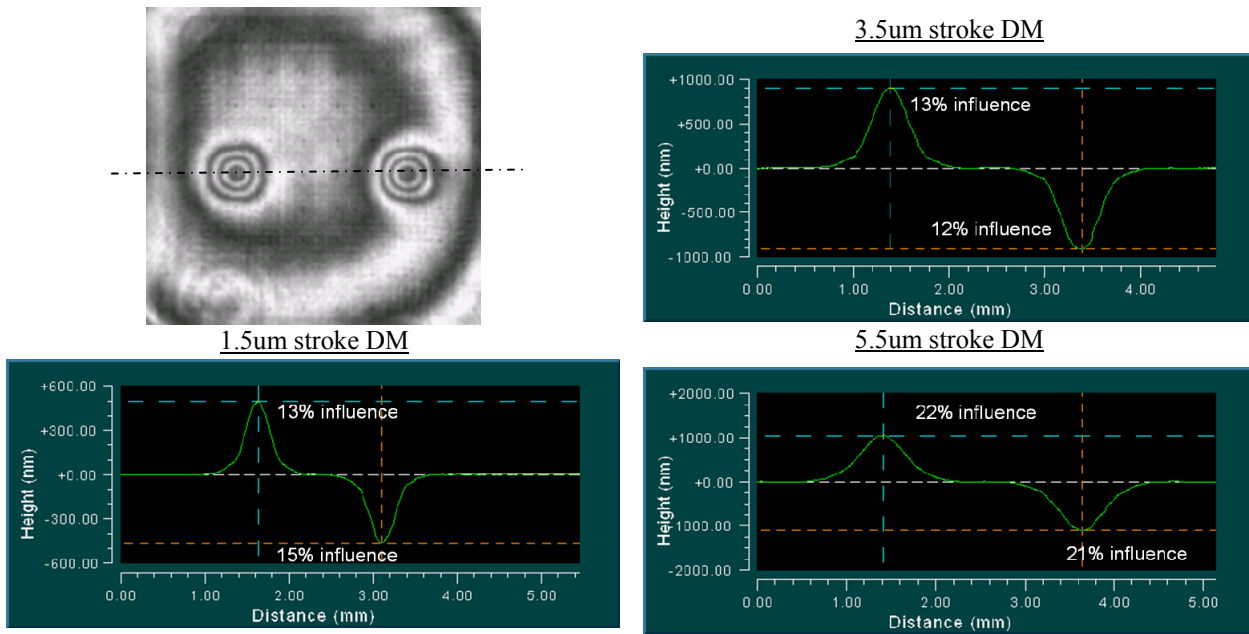


Figure 4. Interferogram of a DM at half bias with an actuator pulled down and another poked upward (top). Profile measurements of 1.5um, 3.5um, and 5.5um actuator stroke DM surfaces show the influence functions of these DM types to be 15%, 13% and 22% respectively.

The inter-actuator stroke for these devices is measured by applying voltage to every other row of actuators estimating a sine wave. A maximum inter-actuator stroke greater than 1.5um can be achieved with the 3.5um stroke DM. Profile cross-sections of each of these DM types is shown in Figure 5.

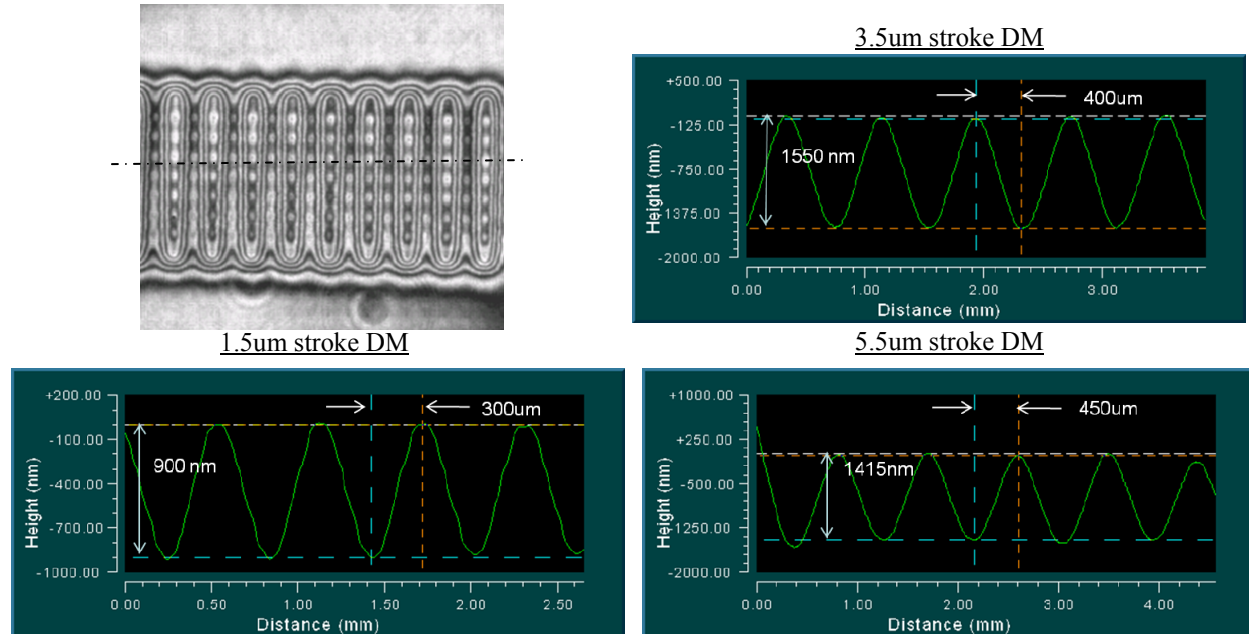


Figure 5. Interferogram of a DM with every other row of actuators actuated (top). Profile measurements of 1.5um, 3.5um, and 5.5um actuator stroke DM surfaces show inter-actuator stroke of these DM types to be 900nm, 1550nm, and 1415nm respectively.

The polysilicon, double cantilever electrostatic actuator designs used in these MEMS DMs presented here are not significantly affected by operating temperatures (Figure 6), do not suffer from fatigue due to cycling (Figure 7), and provide hysteresis free operation (Figure 8). DM actuator cycling and reliability assessment is being performed on a continuous basis [9] and to date DM actuators have been cycled in excess of 20.7 billion cycles without any degradation in electromechanical performance.

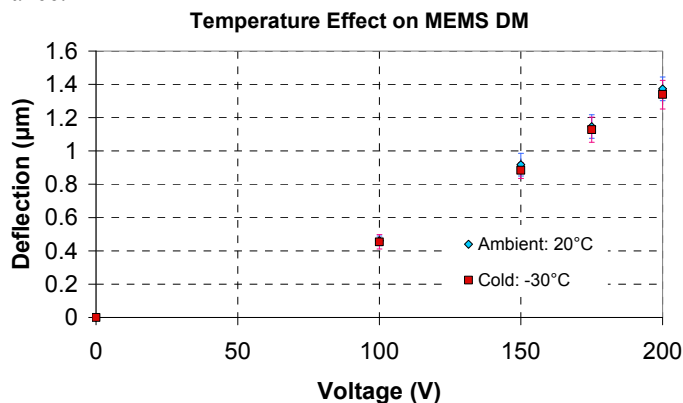


Figure 6. Comparison of the electromechanical performance of a MEMS DM at 20°C and -30°C. No change in this characteristic is measured.

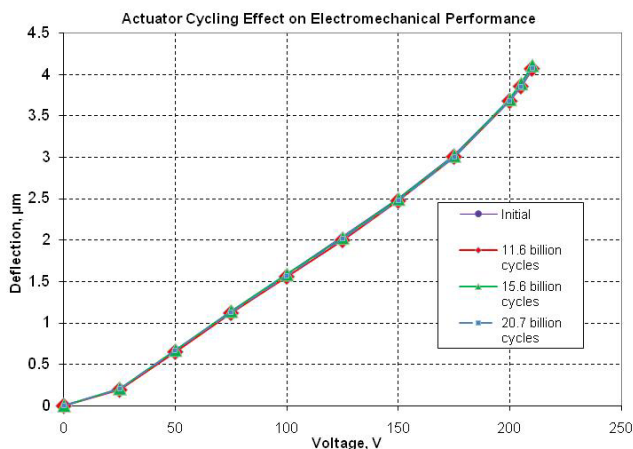


Figure 7. Comparison of DM actuator electromechanical performance before and after actuator cycling. No change in electromechanical performance is measured after 20.7 billion cycles.

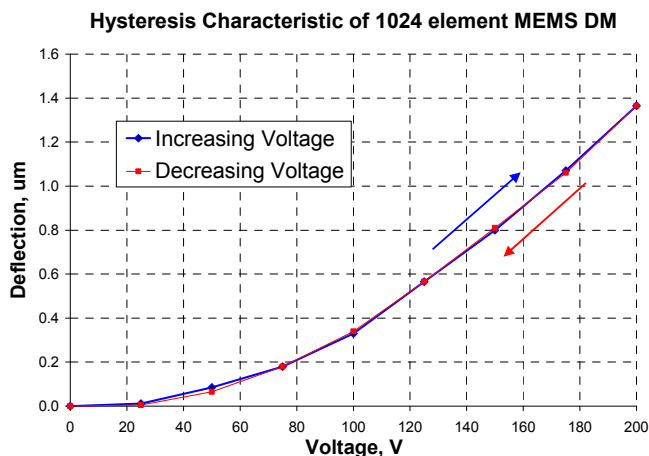


Figure 8. Deflection data of a 1024 element continuous facesheet MEMS DM showing that the electrostatic actuator does not exhibit hysteresis effects (Blue line: increasing voltage, Red line: decreasing voltage)

4. 4092 ACTUATOR DM

4092 actuator continuous facesheet DM has been under development for use in the Gemini Planet Imager. This device, shown in the GPI mount in Figure 9, uses the 3.5 μm stroke DM actuator design and will be used as a tweeter DM in this high contrast imaging instrument to correct for the high order wavefront errors induced by the atmosphere. A woofer DM is used in this instrument to compensate for low-order aberrations. As discussed in section 2, achieving a 100% actuator yield has been the main challenge in this development effort due to the large size of the device and limited number devices processed in the three fabrication runs that have been performed to date. Figure 9 shows both the unpowered surface figure of a typical 4092 actuator DM and a yield chart indicating the number and location of its 38 anomalous actuators. The low-order unpowered surface figure error of these large devices is mainly due to the bow in the silicon substrate on which the DM is fabricated resulting from mismatched film stresses on the front and back side of the silicon wafer. The resulting curvature leads to a peak-to-valley surface figure error of about 4 μm in the active aperture. Although undesirable, most of this low-order error is spherical ($\sim 50\text{m}$ radius of curvature) and astigmatic and may be removed using simple modifications to the optical setup. In the case of a woofer-tweeter setup, this low order error can be mitigated further using the woofer DM as is the case for the GPI for which this DM has been developed. The actuator yield loss has contributed to a handful of microscopic defects that were introduced during the fabrication process and resulting electrical short to ground (dead/weak actuators) or other actuators.

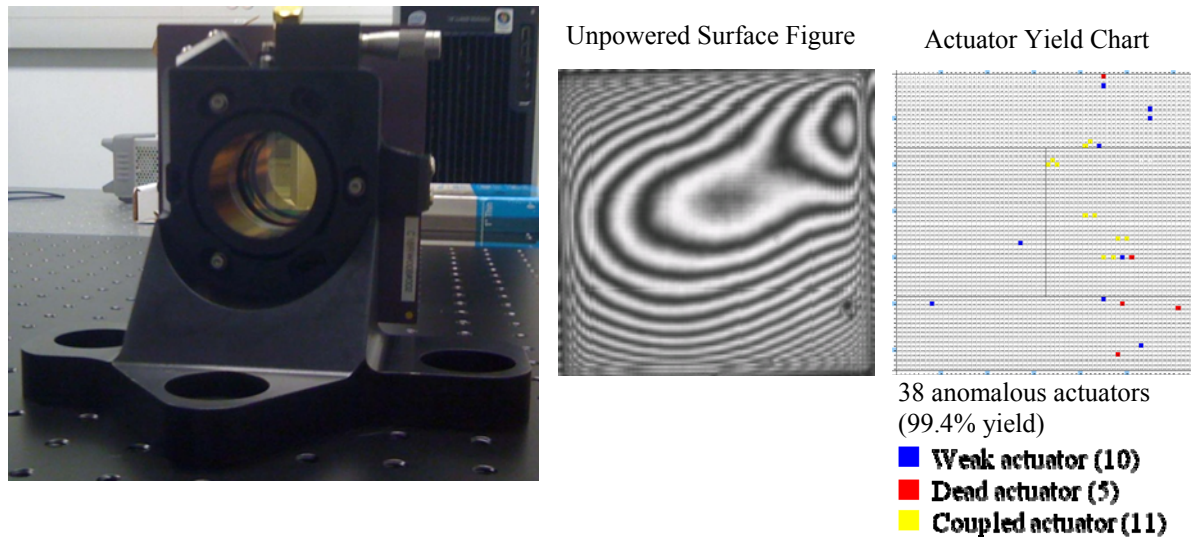


Figure 9. 4092 actuator MEMS DM (Left); Typical unpowered surface figure of DM ($\sim 4\mu\text{m}$ P-V) (Center); Actuator yield chart of device showing 38 anomalous actuators (Right)

To evaluate the DM's ability to correct for the high-order wavefront aberrations expected at the Gemini South Observatory, and to investigate the effects of the anomalous actuators, the DM was controlled to sample wavefront error maps. Since the woofer DM for the GPI instrument has sufficient stroke to compensate for both the low-order atmospheric aberrations and the unpowered surface figure of the DM, the shape of the DM was controlled to a shape in which the unpowered DM figure was added to the wavefront error map to represent the true shape that the DM must take to achieve the desired imaging quality. As shown in Figure 10, the DM was able to match this shape to less than 14nm rms with the 38 anomalous actuators (with these actuators masked out an rms error of less than 3nm rms was achieved – this is within the controller and measurement error of the closed-loop control system used for this experiment).

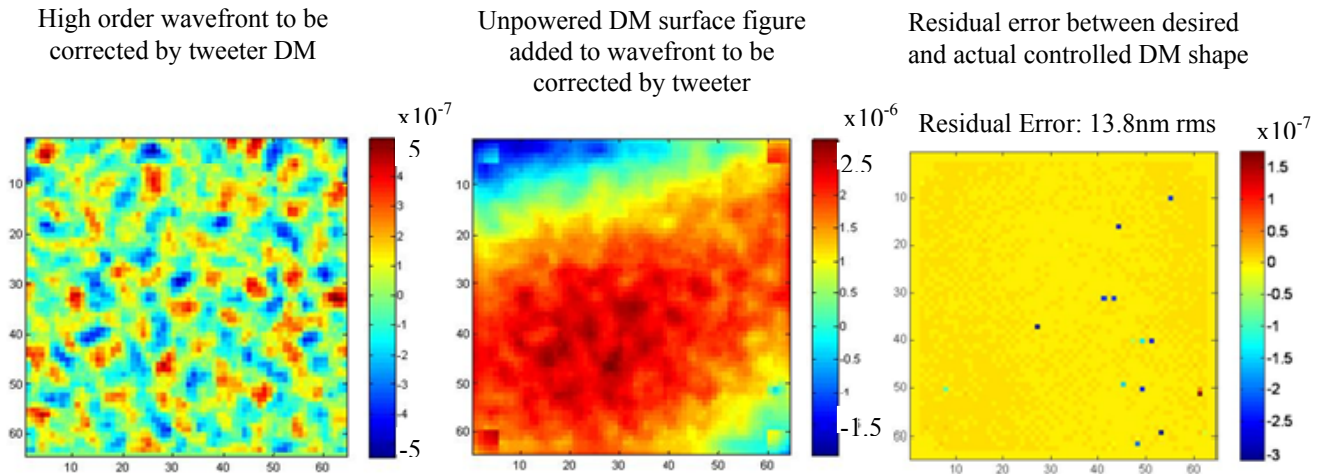


Figure 10. Residual wavefront error after 4092 actuator DM is controlled to a desired shape representative of the high-order atmospheric aberrations to be corrected by the tweeter DM is measured to be 13.8nm rms (right) with 38 anomalous actuators in the aperture. Left: The wavefront to be corrected for using the tweeter DM that remains after the woofer DM has compensated for the low-order errors, including the unpowered tweeter DM surface figure. Center: Actual shape tweeter DM must take to correct for wavefront error (unpowered DM shape added to wavefront error)

5. DM DRIVE ELECTRONICS

A modulator drive electronics system has been developed that can be configured for 128 to 4096 channels (see figure 11 - left), within a single chassis. This compact electronics unit uses high-density flex cables to carry the high-voltage drive signals to the DM. To keep the optical footprint of the DM small, a custom ceramic package was designed to which the DM die is mounted and wire bonded. High density connectors for the 4092 actuator DM are attached directly to the back of the ceramic chip carrier (see figure 10 - right) so that the overall size of the package could remain small – 127mm x115mm.

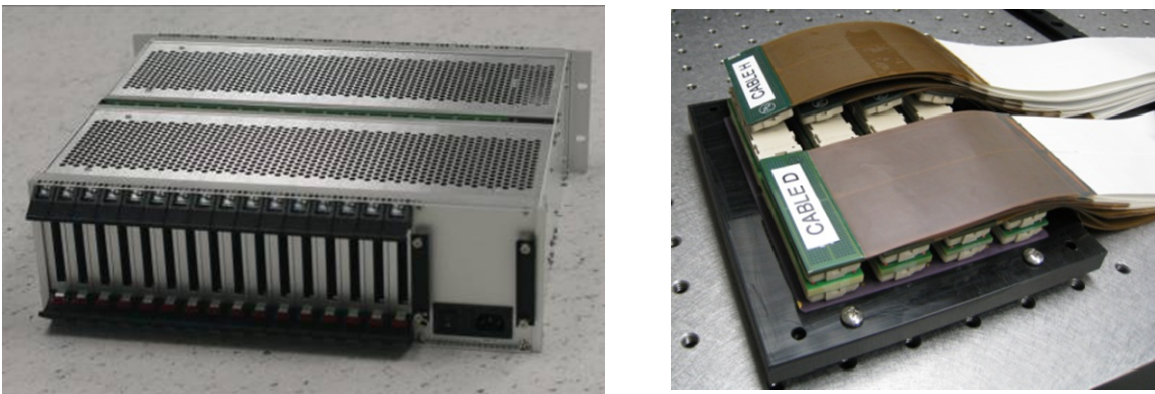


Figure 11. 4096 channel MEMS DM Drive electronics unit (right) designed for the MEMS DMs. The modular design can be configured to drive DMs with 128-4092 actuators and can drive multiple DMs if needed. High density flex cables connect directly to the back of the DM carrier to minimize its size (right)

These electronics can provide 14-bit resolution signals to the DM actuators to achieve sub-nanometer control. Low voltage frame signals are sent to the driver internal FPGA using a 200MB/s, 32-bit LVDS DIO card using a PC. Frame rates in excess of 20kHz, with a latency of 45 μ s, can be achieved for a 4092 actuator DMs. By reconfiguring the driver

boards, a 1020 actuator DM can be driven at frame rates greater than 60kHz, with 15 μ s latency to enable high bandwidth AO controllers.

The drive electronics for a 4092 actuator DM operating at 10kHz consume approximately 120Watts of power. Most of this power is used to power the high voltage supplies and amplifiers since the individual MEMS DM actuators consume only microwatts of power.

A new DM drive electronics architecture is currently under development that will reduce the total power consumption of the DM drive electronics by two orders of magnitude using multiplexing. These electronics will take advantage of the electrostatic actuator's ability to hold its charge to eliminate the need for a single DAC and amplifier for each DM actuator. These next generation electronics, intended for use in space-borne astronomical instruments where small size and low power consumption are very beneficial, will have 16-bit resolution with a goal of achieving <10pm step control of the DM actuators.

6. MEMS DMs WITH >4092 ACTUATORS

The architecture used for the 4092 actuator DM, in which the devices are packaged in a ceramic chip carrier and electrical interconnections are made using wirebonding techniques, can be extended to devices of up to 6082 actuators for DMs with up to 89 actuators across the active aperture. Extending to 6082 actuators will stretch the size of the substrate to the practical limits of current polysilicon surface micromachining processes as well as the wirebonding process. As previously discussed, achieving a 100% actuator yield on a device of this size will require a significant number of fabrication runs to realize. By reconfiguring the actuator layout, DMs with 72 actuators across the active aperture (4092 actuators in the active aperture) can be fabricated using the same substrate size and components as the 64x64 actuator DM (3256 actuators in the active aperture) and we are close to achieving 100% actuator yield on this device.

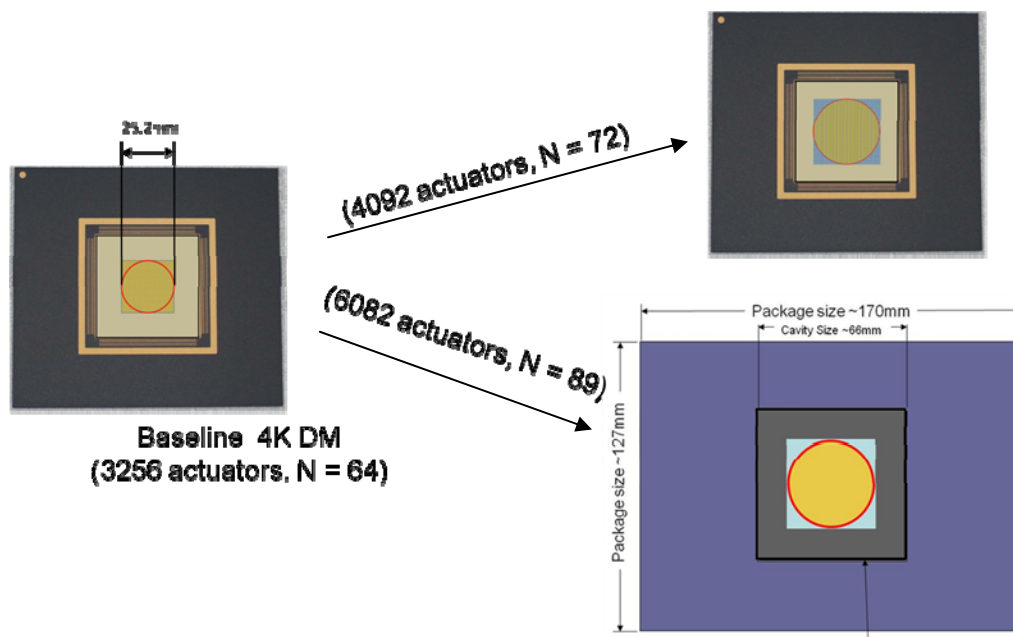


Figure 12. The 64x64 actuator DM (left) with 3256 actuators within the 64 actuator diameter circular aperture may be modified to have 4092 actuators in a circular aperture of 72 actuators across its active aperture (top right). The practical limit of this architecture is a MEMS DM with up to 6082 actuators (89 actuators across) the active aperture (bottom right)

For MEMS DMs of 100x100 or 200x200 actuators as needed for some of the astronomical instruments proposed for the next generation of large telescopes (TMT, E-ELT), a new architecture for making the electrical interconnects is required. The DM design of these devices will be based on the core electromechanical architecture of BMC MEMS DMs, as

presented in the previous sections, that has proven successful in astronomical AO. As illustrated in Figure 13, the significant departure from previous MEMS DM fabrication production techniques is that the DM's electrical interconnections to its high-voltage (HV) driver will be made by integrating an array of high-density through-wafer-vias (TWV) into the MEMS wafer substrate prior to processing. These vias will be used to connect the MEMS device to an underlying "interposer," which will in turn route HV connections to a computer-controlled driver without the need for high-density cabling. By routing interconnections through the wafer instead of fanning them out from the mirror to a peripheral ring of bond pads, the device will be significantly less susceptible to processing defects that constrain DM size in currently used MEMS DM production and packaging. Reducing the overall die size will be required.

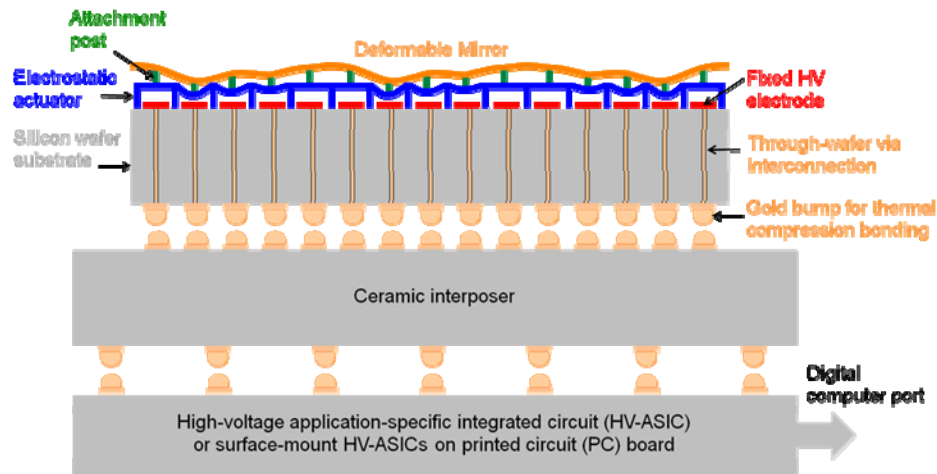


Figure 13, Cross-sectional schematic of MEMS Deformable mirror with through-wafer electrical interconnections to be used for 100x100 to 200x200 actuator devices.

This architecture may be used to directly integrate the DM with multiplexing electronics to eliminate the need for the significant cabling that will be required to carry the DM control signals to the tens of thousands of actuators.

The integration of these through-wafer vias with the DM fabrication process has already been demonstrated by BMC, in collaboration with researchers at Boston University [10]. In this 12x12 DM, actuator arrays were fabricated with through-wafer vias and bump bonded to interposer boards that were used to bring in the drive signals to address the individual actuators.

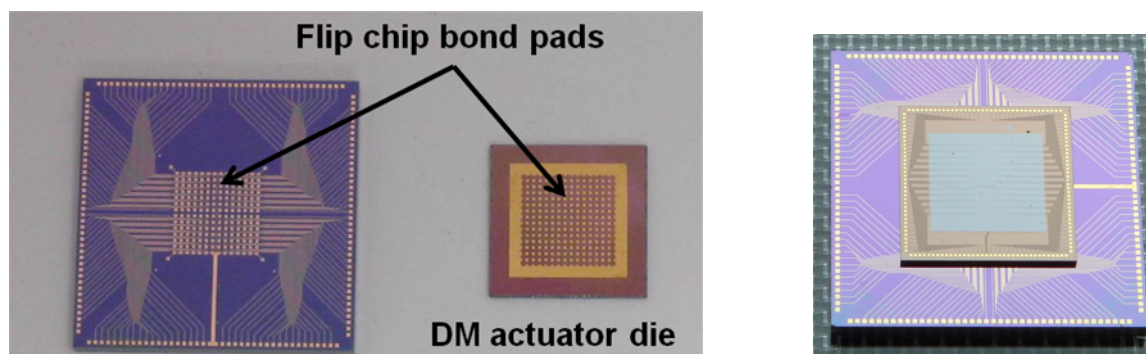


Figure 14, Interposer board and back side of DM actuator die with through-wafer vias (left). Gold bond pad arrays on the interposer die and reverse side of the TWV die (left) to be aligned and bonded using the thermo-compression process (right). Gold bumps are deposited on the interposer bond pads prior to being bonded

7. CONCLUSION

Boston Micromachines has developed a scalable deformable mirror architecture that is well suited for high order aberration correction in astronomical imaging instruments. DMs with 140 and 1020 actuators are routinely fabricated with 100% actuator yield and have proven to be effective and reliable in on-sky wavefront correctors. A 4092 actuator DM with 99.4% actuator yield has also been demonstrated and 100% actuator yield will also be achieved as the fabrication process is refined and repeated. The DM architecture, fabrication process, and drive electronics can practically be scaled to about 6000 actuator DMs. For MEMS DMs with tens of thousands of actuators, a new electrical interconnect scheme will be required using through-wafer via interconnection that has been demonstrated and shown to be feasible in pilot programs.

REFERENCES

1. Donald Gavel, Mark Ammons, Brian Bauman, Daren Dillon, Elinor Gates, Bryant Grigsby, Jess Johnson, Chris Lockwood, Kathleen Morzinski, David Palmer, Marc Reinig, and Scott Severson, *Visible light laser guidestar experimental system (Villages): on-sky tests of new technologies for visible wavelength all-sky coverage adaptive optics systems*, Proc. SPIE 7015, 70150G (2008)
2. Donald T. Gavel, *Progress update on the visible light laser guidestar experiments at Lick Observatory*, Proc. SPIE 7595, 759508 (2010)
3. C. Baranec, R. Dekany, S. Kulkarni, N. Law, E. Ofek, M. Kasliwal & V. Velur, *"Deployment of low-cost replicable laser adaptive optics on 1-3 meter class telescopes,"*, Astro2010: The Astronomy and Astrophysics Decadal Survey, 2009.
4. Bruce Macintosh, James Graham, Ben Oppenheimer, Lisa Poyneer, Anand Sivaramakrishnan, and Jean-Pierre Veran, *MEMS-based extreme adaptive optics for planet detection*, Proc. SPIE 6113, 611308 (2006)
5. Bruce A. Macintosh, James R. Graham, David W. Palmer, René Doyon, Jennifer Dunn, Donald T. Gavel, James Larkin, Ben Oppenheimer, Les Saddlemyer, Anand Sivaramakrishnan, J. Kent Wallace, Brian Bauman, Darren A. Erickson, Christian Marois, Lisa A. Poyneer, and Remi Soummer, *The Gemini Planet Imager: from science to design to construction*, Proc. SPIE **7015**, 701518 (2008)
6. Andrew Norton, Julia Evans, Donald Gavel, Daren Dillon, Dave Palmer, Bruce Macintosh, Katie Morzinski, Steven Cornelissen, *Preliminary characterization of Boston Micromachines' 4096-actuator deformable mirror*, MEMS Adaptive Optics III. Proceedings of the SPIE, Volume 7209 (2009)., pp. 72090I-72090I-7 (2009).
7. B.M. Levine, M. Shao, D. Liu, J.K. Wallac, B. Lane, *Planet Detection in visible light with a single aperture telescope and nulling coronagraph*, Proc. SPIE 5170 (2003) 200-208
8. B.M. Levine, M. Shao, C.A. Beichman, B. Mennesson, R. Morgan, G. Orton, E. Serabyn, S. Unwi, T. Velusamy, N. Woolf, *Visible light terrestrial planet finder – planet detection and spectroscopy by nulling interferometry with a single aperture telescope*, Proc SPIE (2003) 221-229.
9. Allyson L. Hartzell, Steven A. Cornelissen, Paul A. Bierden, Charlie V. Lam, and Daniel F. Davis, *Reliability of MEMS deformable mirror technology used in adaptive optics imaging systems*, Proc. SPIE 7595, 75950B (2010)
10. Alioune Diouf, Thomas G. Bifano, Jason B. Stewart, Steven Cornelissen, and Paul Bierden, *Through-wafer interconnects for high degree of freedom MEMS deformable mirrors*, Proc. SPIE 7595, 75950N (2010)